

Performance Comparison of R1233zd(E) and R515B for Two-Phase Direct-to-Chip Cooling

Qingyang Wang^{1,*}, Akshith Narayanan¹, Serdar Ozguc¹, Jacob D. Moore¹, Richard W. Bonner III¹
¹Accelsius, Austin, TX, USA
*qwang@accelsius.com

Abstract: As the power density of high-performance processors continues to increase with the advancement of artificial intelligence, traditional air convection can no longer keep up with the cooling demand for data centers. Liquid cooling technology with higher capacity and efficiency plays a crucial role in enabling continued development and application of artificial intelligence technologies, in which two-phase (2P) direct-to-chip (DTC) cooling has demonstrated impressive performance and holds a promising future. Various types of dielectric refrigerants have been used for 2P cooling, each offering different properties and advantages. In this work, we conducted experiments on a thermal test loop with two different types of thermal test vehicles (TTVs) representing a CPU (Intel Sapphire Rapids) and a GPU (Nvidia H100), respectively. 2P cooling cold plates developed for these processors are tested under varying conditions. Two different refrigerants are used, including a low-pressure refrigerant R1233zd(E) and a medium-pressure refrigerant R515B. The results show that both refrigerants exhibit flow rate-independent performance in the 2P cooling regime within wide vapor quality ranges. Compared with R1233zd(E), R515B yields smaller thermal resistance for the cold plate on the CPU TTV and similar thermal resistance for the cold plate on the GPU TTV. R515B also causes lower pressure drop across the quick-disconnect coupling at given flow rates and heat loads. On the other hand, R1233zd(E) has much lower global warming potential (1 vs 293), and its low pressure allows for eased mechanical requirements for system components, while also offering sufficient cooling performance. This work provides a performance comparison between an eco-friendly refrigerant and a high-performance refrigerant in 2P DTC cooling, and offers insights for 2P cooling adopters in selecting working fluids based on their prioritized considerations.

Keywords: two-phase, direct-to-chip, data center cooling, thermal test vehicle, thermal resistance

I. INTRODUCTION

The rapid development of artificial intelligence and machine learning technologies leads to a surging demand for high-performance computing. High-performance CPUs, GPUs, and AI accelerators are being developed with increasingly high thermal design power (TDP) and heat flux. Meanwhile, the processors and servers are being packed with higher density in server racks and data centers. Traditional data centers relying on air cooling will struggle to meet the cooling requirements, and liquid cooling solutions with high performance and high efficiency are becoming a necessity. Single-phase (1P) direct-

to-chip (DTC) using water/propylene glycol-based coolant has been employed to address the chip-level, server-level, and rack-level high power densities, and offers superior cooling performance compared to air cooling [1]. As the TDP and heat flux of the processors are projected to keep increasing, thermal management solutions using two-phase (2P) heat transfer are considered promising due to the high heat transfer efficiency of boiling and the high heat transfer capacity offered by the latent heat of a fluid.

2P heat transfer has been widely studied in the academic community, with lab-scale experiments demonstrating ultrahigh heat flux using both water [2-4] and dielectric fluids [5, 6]. 2P DTC technology implements the high cooling performance of liquid-vapor phase change, and allows dissipation of high TDP over 2.2 kW [7] and high heat flux over 300 W/cm² [8] at the processor-level. Kulkarni et al. [9] provided a comprehensive introduction of 2P DTC technology. A 2P DTC system is similar to a 1P DTC system, except an additional reservoir is needed in the loop to accommodate the volume expansion of liquid-vapor phase change process during operation. It is demonstrated that a universal cold plate concept is feasible, where when a 1P DTC cold plate is run in 2P mode with refrigerant, 2P mode offers better performance than 1P mode even without optimizing the cold plate for 2P [8, 10], allowing data centers with existing 1P DTC systems to easily transition to 2P DTC using shared components without sacrificing cooling performance. 2P DTC is versatile to operate under different orientations and enable different server packaging designs [11], and offers great reliability as the use of dielectric fluids prevents bio growth, corrosion, and disastrous IT equipment damage when leakage occurs.

Various types of refrigerants exist as potential candidates for 2P DTC working fluids. Karwa et al. [12] introduced a low-pressure refrigerant R1233zd(E) with ultralow GWP, achieving a lower junction temperature compared to 1P water. Wang et al. [13] demonstrated high cooling performance using R1233zd(E) in server-level experiments. Heydari et al. [14] analyzed different refrigerants for 2P DTC and compared with a conventional refrigerant, providing discussions on various considerations. Kulkarni et al. [8] showed a medium-pressure refrigerant R515B demonstrating lower thermal resistance than 1P PG25 on multiple thermal test vehicles (TTVs). While all

these refrigerants provide great thermal performance in 2P DTC cooling, different refrigerants offer different properties and advantages. A comparison of the thermohydraulic performance of different refrigerants would provide important information for data centers to choose different working fluids for 2P DTC cooling.

In this work, we conducted experiments on a server-level experimental test loop with two different TTVs representing a high-performance CPU and GPU, respectively. Two types of refrigerants are tested, including a low-pressure refrigerant R1233zd(E) and a medium-pressure refrigerant R515B. The thermohydraulic characteristics are analyzed and discussed. It is found that both refrigerants demonstrate flow rate-independent performance in the 2P cooling regime when nucleate boiling is fully developed. Compared to R1233zd(E), R515B results in a smaller thermal resistance for the CPU TTV and a similar thermal resistance for the GPU TTV. R515B also yields a lower pressure drop across the quick-disconnect (QD) coupling at given flow rates and heat loads. On the other hand, R1233zd(E) relieves the mechanical requirements for high-pressure rating and offers an ultralow GWP of 1, making it preferable for mechanical and environmental considerations. Our work comprehensively compares two readily available refrigerants with different operating pressures for 2P cooling, and provides valuable insights into the selection and deployment of 2P DTC cooling technology.

II. EXPERIMENTAL

A. Thermal Test Loop

The thermal test loop of this work is the same as the one used in previous works [7, 10, 13, 15], except a second loop is established to accommodate the two different working fluids, avoiding time-consuming draining/refilling and cross-contamination of different refrigerants. Fig. 1 shows the schematic of the test loop, consisting of a condenser, a reservoir, a gear pump, and a test sled. Flexible hoses, stainless steel tubes, and high-pressure flexible tubes are used to hydraulically connect different components of the loop. In the test sled, TTVs are used to generate prescribed heat loads and mimic a real high-power processor. In this work, a single TTV is used for each experiment as shown in Fig. 1. Two types of TTVs are designed and investigated in this work, conforming to the form factors of two widely used processors in the industry, namely, the Sapphire

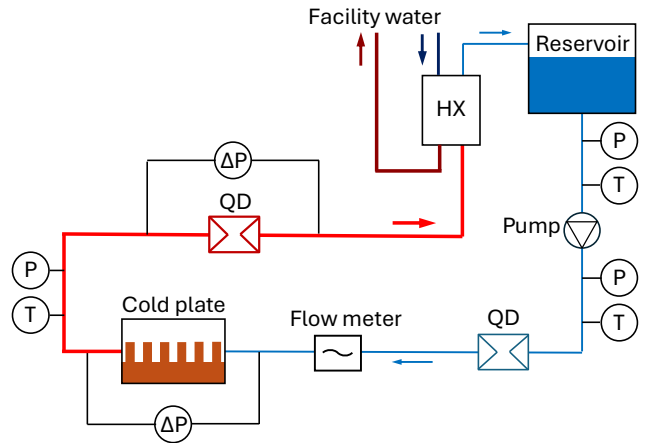


Fig. 1. Schematic of the experimental system.

Rapids CPU from Intel and the Hopper H100 GPU from Nvidia. The details of the TTVs are presented in following sections. Skived copper cold plates designed for these two processors are attached onto the TTVs with a phase-change based thermal interface material (TIM) sandwiched in between. The TIM is compressed with the same pressure during all tests on a given TTV to ensure consistent TIM performance. Thermocouples (TCs) and pressure sensors are placed at the exit of the reservoir, downstream of the pump, and at the outlet of the cold plates. The pressure drop across the cold plate and across the vapor QD coupling and its connecting hoses are measured using differential pressure sensors. The fluid volumetric flow rate is measured using a clamp-on ultrasonic flow meter. Heating power is applied to the heaters in the TTVs to simulate heat generation from the processors. TCs are also implemented in the TTVs to obtain the case temperature. Measurement data are collected using a commercial data acquisition unit with a 1-second interval. In each experimental condition, measurements are taken for ~ 1 min to ensure steady-state has been reached, and each quantity (temperature, pressure, pressure drop, flow rate) is averaged for at least 10 seconds in the steady-state period. Measurement uncertainties can be found in Ref. [13].

B. Thermal Test Vehicles

Fig. 2a-b shows a photo and the drawing of the TTV used for Intel Sapphire Rapids CPU, named TTV1 hereafter. Four ceramic heaters with a power capacity of 250 W each are used

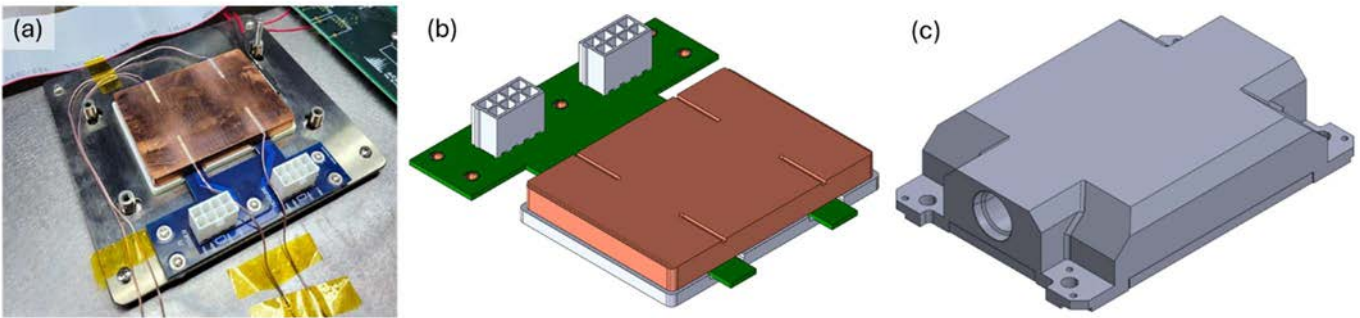


Fig. 2. Photo (a) and drawing (b) of the TTV1 and its corresponding cold plate (c).

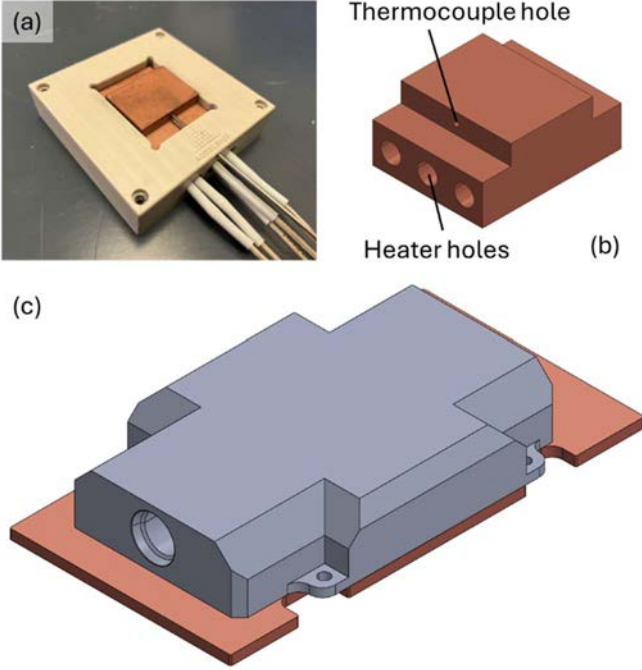


Fig.3. Photo (a) and drawing (b) of the TTV2 and its corresponding cold plate (c).

to generate heat, which are powered by supplying DC voltage. The bottom sides of the heaters are insulated, and the top sides are enclosed by an integral heat spreader made of copper with thermal grease applied in between to ensure good thermal contact. The top surface of the integral heat spreader has a size matching the Sapphire Rapids chip package. Four TC grooves are machined on the top surface of the heat spreader, and T-type TCs are embedded in the grooves using epoxy. The TC grooves are positioned such that the TC junctions are measuring the case surface directly on top of the heaters. Fig. 2c shows a CAD drawing of the corresponding cold plate designed for the chip package and tested on TTV1.

Fig. 3a-b shows a photo and the 3D CAD model of the TTV used for Nvidia H100 GPU, named TTV2. TTV2 is made from a copper block with a heating surface area (the top surface area) matching the die of an H100 chip. It is noted that the actual H100 chip has memory components generating some amount of power, but the TTV2 with only the die area heated ensures conservative conclusions by assuming all the heat is dissipated through the die area. Therefore, with a TTV2 power matching the TDP, the cold plate is cooling a higher heat flux than in practical conditions. To generate heating power, three cartridge heaters are inserted into the base block of the TTV2. The bottom and side surfaces of the TTV2 is thermally insulated by a PEEK block. A 0.8 mm diameter hole is drilled halfway through the width of the heating area, with its centerline 3.175 mm below the heating surface. A K-type TC probe is inserted into the hole, so that the tip of the probe is right at the center of the heating area. The case temperature is then obtained from the TC measured temperature by assuming uniform 1D heat conduction across the narrowed section of TTV2. Fig. 3c shows the CAD

TABLE I. LIST OF PROPERTIES FOR R1233zd(E) AND R515B

Properties	Unit	R1233zd(E)	R515B
Global warming potential	-	1	293
Normal boiling point (@101.3 kPa)	°C	18.3	-18.9
Critical temperature	°C	165.5	108.7
Density @25 °C	Liquid	kg/m ³	1262.8
	Vapor		7.2
Viscosity @25 °C	Liquid	μPa·s	286.0
	Vapor		10.3
Specific heat @25 °C	Liquid	kJ/kg·K	1.22
	Vapor		0.83
Thermal conductivity @25 °C	Liquid	mW/m·K	82.7
	Vapor		10.7
Latent heat @25 °C	kJ/kg	191.2	141.3
Surface tension @25 °C	mN/m	14.6	8.8
Saturation pressure @25 °C	psi	18.8	72.1
Saturation pressure @50 °C	psi	42.6	144.7

drawing of the corresponding cold plate designed for H100 chips and tested on TTV2.

C. Refrigerants

Different refrigerants have been studied for 2P DTC cooling. Based on their working pressure, they can be categorized into low-pressure, medium-pressure, and high-pressure refrigerants. Low-pressure and medium-pressure fluids are most considered for 2P DTC cooling. In this work, we choose one refrigerant from each category: a low-pressure refrigerant R1233zd(E), and a medium-pressure refrigerant R515B. Table 1 shows the representative properties of the two fluids used in this study.

D. Data Reduction

For a given test condition, the cold plate exit vapor quality and thermal resistance are calculated from directly measured parameters. The exit vapor quality is calculated as

$$x = \frac{Q_{tot} - Q_{sens}}{\rho_l \dot{V} h_{fg}} \quad (1)$$

Here, \dot{V} is the measured liquid volumetric flow rate. Q_{tot} is the total heat load, and Q_{sens} is the sensible heat portion due to inlet subcooling, obtained by

$$Q_{sens} = \rho_l \dot{V} c_p (T_{sat} - T_{in}) \quad (2)$$

where T_{sat} is the saturation temperature inside the cold plate and is taken as the measured outlet temperature of the cold plate (assuming minimal pressure drop from the cold plate to the outlet [16]), and T_{in} is the inlet temperature of the cold plate and is taken as the measured fluid temperature after the pump (assuming negligible heat loss along the fluid tube/hose). ρ_l , h_{fg} and c_p are the liquid density, latent heat of vaporization, and specific heat capacity, respectively.

The thermal resistance is defined as

$$R_{th} = \frac{T_{case} - T_{sat}^*}{Q_{tot}} \quad (3)$$

which is a case-to-fluid lumped resistance including the contributions from TIM, base plate conduction, and boiling/convection. As discussed in Section II-B, TCs are placed differently for two different TTVs. For TTV1, four TCs measure the case temperature directly as they are positioned on the surface, so T_{case} is obtained as the average of the four TC readings. For TTV2, the TC probe is placed below the surface, and the T_{case} is obtained from the measured probe temperature T_{TC} ,

$$T_{case} = T_{TC} - \frac{Q_{tot} \delta}{A k_{Cu}} \quad (4)$$

where A is the cross-sectional area of the 1D heat conduction segment of the TTV2, δ is the distance from the TC probe to the TTV2 surface (3.175 mm), and k_{Cu} is the thermal conductivity of solid copper. The adjusted saturation temperature T_{sat}^* in Eq. (3) is obtained as

$$T_{sat}^* = \frac{Q_{sens} T_{in} + T_{sat}}{2} + \frac{Q_{tot} - Q_{sens}}{Q_{tot}} T_{sat} \quad (5)$$

which incorporates heat transfer contributions from both subcooled 1P liquid convection and 2P boiling.

III. RESULTS AND DISCUSSION

A. Effect of Flow Rate

Experiments are conducted with both TTVs to investigate the effect of flow rate. Fig. 4 shows the performance curves of the cold plate on TTV1, plotted as the thermal resistance as a function of heating power, with Fig. 4a showing curves for R1233zd(E) and Fig. 4b showing curves for R515B. The heat loads are ramped from 100 to 1000 W under a given flow rate for both fluids, and three different flow rates are tested for each fluid. It can be seen that at lower power levels (100&200 W for R1233zd(E) and 100 W for R515B), the thermal resistance varies with flow rate, but with no obvious and clear correlation; higher flow rate does not always result in higher or lower thermal resistance. This can be attributed to the random nature of boiling incipience and multiple counter acting effects: a higher flow rate results in higher heat transfer coefficient (HTC) before boiling incipience when the cooling mode is 1P convection only; on the other hand, with a given heating power, a higher flow rate results in more 1P contribution, which has lower HTC compared to boiling, and causes delayed boiling incipience than lower flow rate conditions. When the heating power reaches 300 W for R1233zd(E) and 200 W for R515B, the effect of flow rate becomes negligible, which is due to the dominance of boiling heat transfer over convection after nucleate boiling has been fully developed. Slight difference between curves is still present due to the potential variation in TIM conditions as well as the experimental systematic error among different tests.

Fig. 5 shows the experimental results obtained on TTV2 and its corresponding cold plate. Different refrigerant flow rates are supplied, which yield different vapor qualities. Fig. 5a shows the thermal resistance as a function of the supplied refrigerant flow rate for both fluids at a fixed heat load of 700 W (TDP of H100).

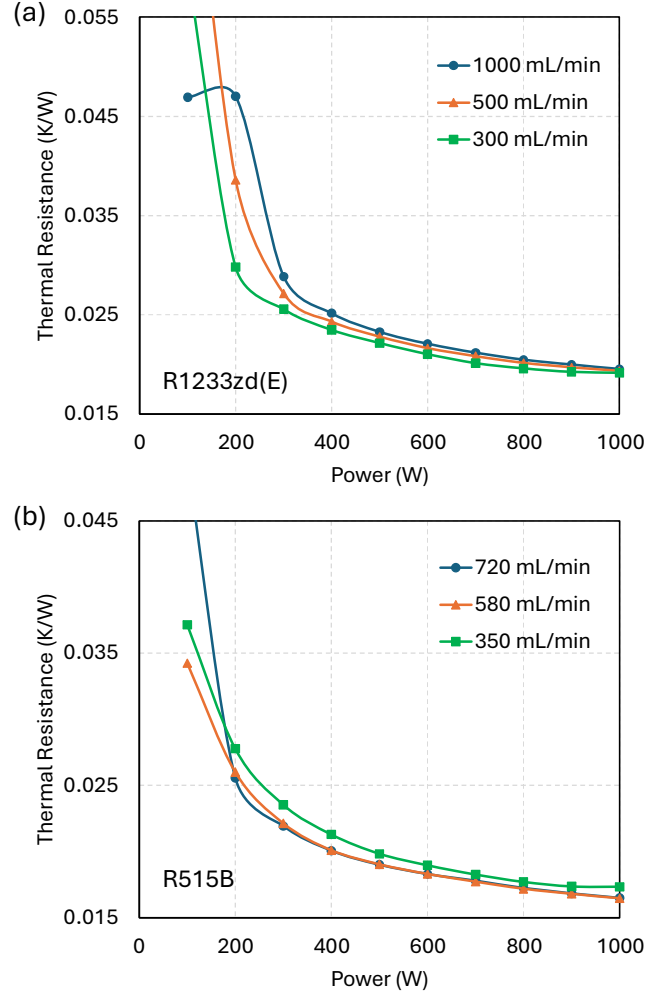


Fig. 4. Thermal resistance variation with heating power obtained on TTV1 with (a) R1233zd(E) and (b) R515B.

For R1233zd(E), the thermal resistance first decreases with increasing flow rate and then increases, and the reason can be well understood when the thermal resistance is plotted against the exit vapor quality as shown in Fig. 5b. The thermal resistance first decreases with increasing exit vapor quality from 0.1~0.3, which is due to reduced 1P contribution. With a fixed power of 700 W, a higher flow rate results in lower exit vapor quality. It also results in a higher pressure drop from the cold plate to the reservoir, therefore causing more inlet subcooling. Consequently, under a higher flow rate and a lower exit quality, a larger fraction of the cooling is contributed by 1P convection of liquid refrigerant (Eq. (2)), which has low thermal performance due to the poor thermophysical properties of liquid refrigerant. When the exit vapor quality is in the range of 0.3~0.7, the thermal resistance remains almost constant, which is due to the dominance of nucleate boiling over forced convection such that the variation of flow rate makes negligible differences. When the exit vapor quality reaches 0.7, the thermal resistance increases with exit quality quickly, which could either be departure from nucleate boiling, or partial dry-out caused by

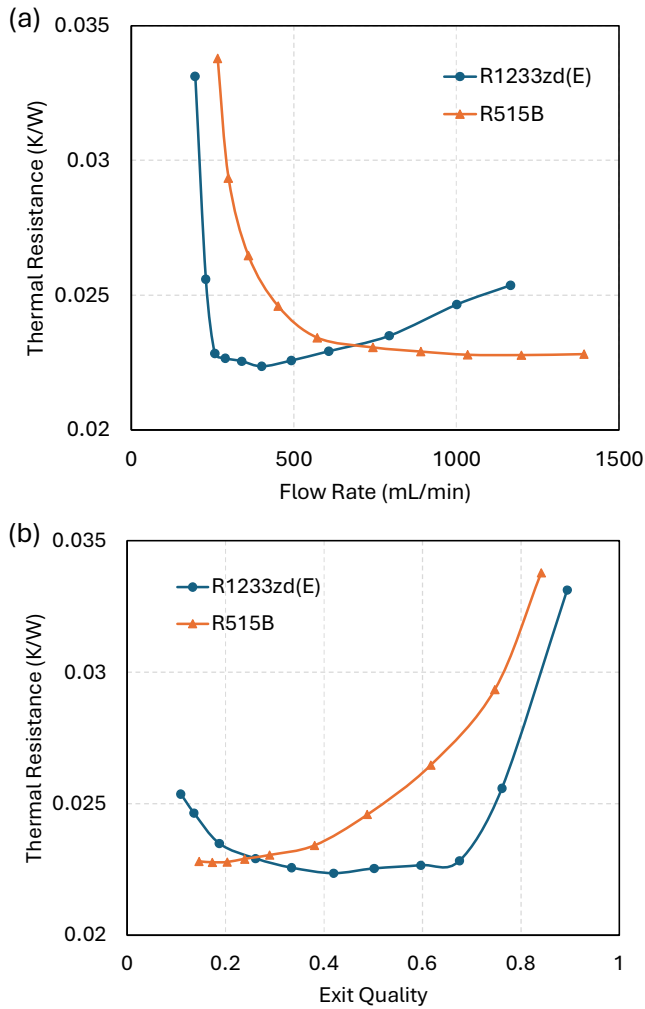


Fig. 5. Thermal resistance variation with (a) flow rate and (b) exit vapor quality for both fluids, obtained on TTV2.

flow instabilities, which are widely observed for flow boiling at high vapor quality conditions [17].

For R515B, the curves in Fig. 5 have a generally similar trend compared to R1233zd(E). The difference is that the increase of thermal resistance at high flow rate and low vapor quality conditions are not shown in the figure. It is likely because R515B with higher vapor density results in lower vapor pressure drop (as discussed in Section III-C below), which causes a very small inlet subcooling. Therefore, even with high flow rates and low vapor exit qualities, the 1P contribution (Eq. (2)) is still small and nucleate boiling contribution can still be dominant given the 700 W heat load. The deterioration of heat transfer occurs at a lower vapor quality condition, which is possibly resulted from errors in flow rate measurement: due to the lower density and lower latent heat of R515B (see Table 1) and its lower pressure drop, it is more likely to cavitate at the pump, causing the ultrasonic clamp-on flow meter to read a higher flow rate than the actual value, corresponding to a lower apparent vapor quality than the real value. Future experiments are needed to calibrate the flow meter and conduct more systematic tests.

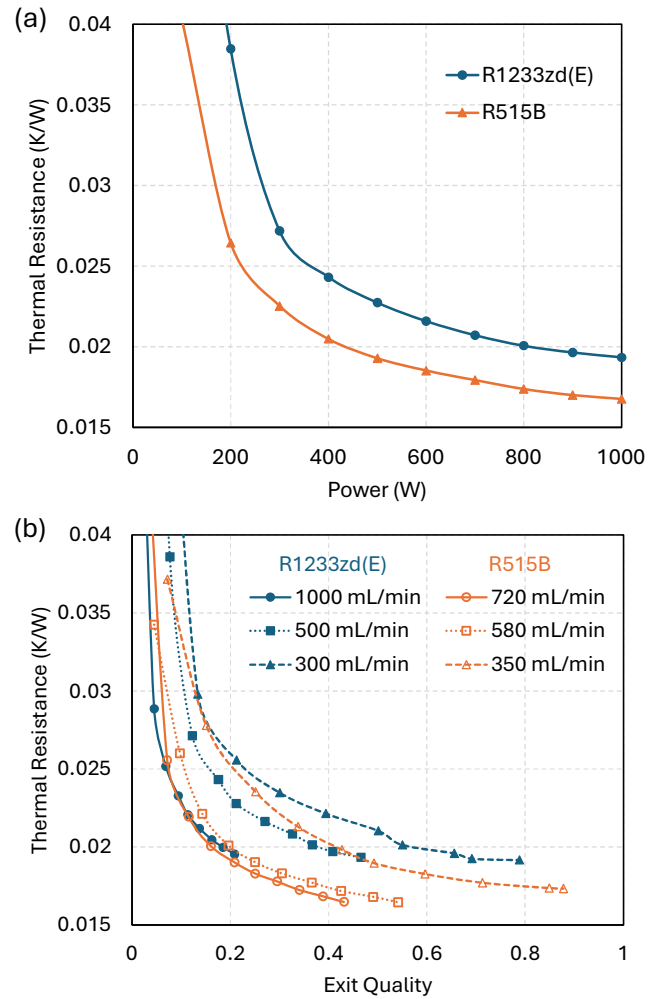


Fig. 6. Thermal resistance as a function of (a) power and (b) exit vapor quality for both fluids. The curves in (a) are the average of three curves shown in Fig. 4 for respective fluids. Data obtained on TTV1.

B. Thermal Performance

Fig. 6 shows the thermal performance of the two fluids tested on TTV1 with the corresponding cold plate. Fig. 6a plots the curves of thermal resistance as a function of power, where for both fluids, the curves are the average thermal resistance of the three flow rate conditions shown in Fig. 4, since flow rate does not cause significant difference as discussed in Section III-A. R515B shows a lower thermal resistance than R1233zd(E) with a given power, indicating a higher boiling HTC. This is consistent with Ref. [10] showing better thermal performance for R515B than R1233zd(E) on the same TTV, and is likely due to the smaller subcooled 1P contribution for R515B. Fig. 6b shows the curves of thermal resistance as a function of exit vapor quality for both fluids with three different flow rates. In general, the resistance decreases with increasing exit quality due to the increased nucleate boiling HTC with higher supplied power (and thus heat flux). The curves do not show deterioration up to an exit vapor quality of ~ 0.9 , because the heat flux on TTV1 was low and departure from nucleate boiling did not occur. Dry-out

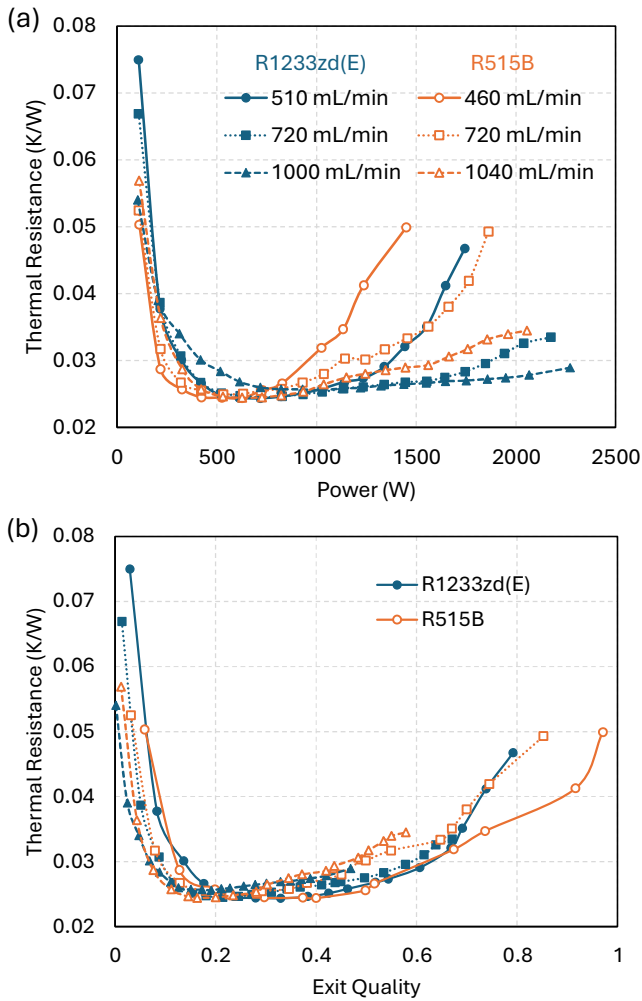


Fig. 7. (a) Thermal resistance as a function of (a) power and (b) exit vapor quality for both fluids with different flow rates. Data obtained on TTV2.

conditions were not tested to protect the ceramic heaters of the TTV from overheating and damage.

Fig. 7 shows the thermal performance of the two fluids tested on TTV2. For each fluids, three flow rates were supplied. As shown in Fig. 7a, the thermal resistance decreases with increasing power at low power conditions due to reduced 1P contribution and nucleate boiling being fully developed. The thermal resistance remains almost unchanged with varying power, with the curves being almost flat, which is due to the dominance of fully developed nucleate boiling. In consistent with Section III-A, the flow rate has minimal effect in thermal resistance when boiling is fully developed. However, the flow rate changes the power at which the curves start to rise at higher power ranges, indicating deteriorated heat transfer. The reason is again due to departure from nucleate boiling or partial dry-out at higher vapor qualities. Fig. 7b shows the curves plotted against the exit vapor quality. The curves consistently show heat transfer deterioration at a similar vapor quality range around 0.5~0.7. Therefore, it is advisable to maintain the exit quality to be below 0.7 when designing operating conditions.

Different from the results in Fig. 6 for TTV1, in Fig. 7 for TTV2, the thermal resistance values for the two fluids have negligible difference under the fully developed boiling conditions, which is likely due to the dominance of conduction (from TIM and copper base plate). Using a simplified 1D analysis, conduction contributes to ~60% or higher in the total thermal resistance. Consequently, even a 10% improvement in HTC from R1233zd(E) to R515B would only cause <4% change in thermal resistance, which could be within the systematic uncertainty of different TIM conditions between tests.

Another difference between the curves tested on TTV1 (Fig. 6) and TTV2 (Fig. 7) is that the curves in Fig. 6 do not show any trend of heat transfer deterioration up to an exit quality of 0.9, while the curves in Fig. 7 start to show deterioration at an exit quality of 0.5~0.7. This is because of the higher heat flux produced by TTV2 due to the much smaller footprint area of TTV2. The heat flux for TTV1 is difficult to estimate due to the existence of a heat spreader, but the cold plates for TTV1 have a much larger boiling area compared to cold plates TTV2. Assuming perfect heat spreading, at an arbitrary heat load of 1000 W, TTV1 produces a heat flux of ~37 W/cm² and TTV2 produces a heat flux of over 110 W/cm². The higher heat flux condition makes it more prone to departure from nucleate boiling and flow instabilities, which requires advanced studies for optimized channel geometries in the future.

C. Pressure Drop

Pressure drop in a pumped 2P system determines the saturation temperature at the cold plate level and requires detailed attention. As shown in Fig. 1, a differential pressure sensor is used to capture the pressure drop of the 2P mixture flowing across the vapor QD coupling along with the hose attached to it. Fig. 8 shows the measured pressure drop as a function of vapor exit quality under different working conditions with the two working fluids. The pressure drop increases with exit quality due to the high pressure drop of vapor phase. It is shown that for a similar value of liquid refrigerant flow rate,

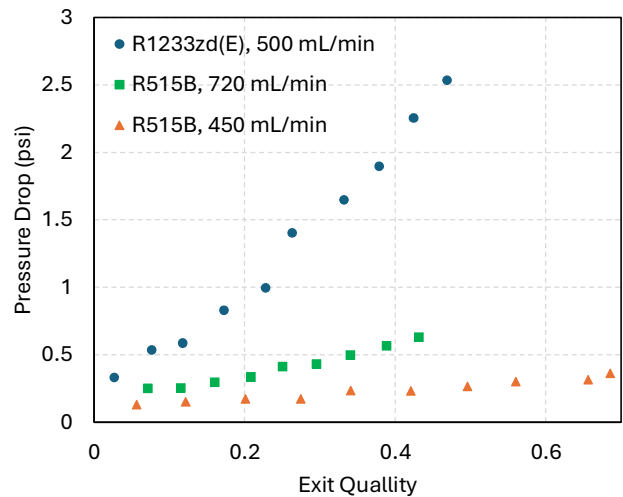


Fig. 8. Measured pressure drop across the vapor hose and QD for the two fluids with different flow rate conditions.

R515B results in a significantly smaller pressure drop than R1233zd(E). Even when R515B has a higher liquid flow rate, it still results in a smaller pressure drop than R1233zd(E) with a lower liquid flow rate. This is due to the much higher vapor density of R515B, as pressure drop decreases with increasing density with a given flow rate. A lower pressure drop for R515B would cause smaller pressure drops in various components of the system including QDs, tubings/hoses, manifolds, and heat exchangers. Therefore, using R515B with high vapor density would require less bulky vapor return tubes/hoses, less powerful pumps, and allows less possibility of 2P flow maldistribution [18, 19]. However, it would also demand more mechanical strength on the system components, as the working pressure at the cold plate increases from 42.6 psi for R1233zd(E) to 144.7 psi for R515B at 50 °C saturation temperature. This difference would be even more prominent with the 3X burst pressure design requirements considering the gauge pressure instead of the absolute pressure. Also, R1233zd(E) has a GWP of 1 compared with R515B with a GWP of 293, which makes it preferable for environmental considerations with sufficiently high performance. Therefore, the two fluids offer different advantages while providing high cooling performance, and data center decision makers can choose between them by prioritizing different considerations.

IV. CONCLUSIONS

2P DTC cooling offers high thermal performance and cooling capacity, allowing efficient and reliable thermal management of advanced and next-generation high power data centers. Various dielectric refrigerants exist for 2P DTC systems, each offering different advantages and meeting different requirements. In this work, we conducted server-level experiments with two TTVs representing two high-performance processors, using both a low-pressure refrigerant R1233zd(E) and a medium-pressure refrigerant R515B. The thermohydraulic characteristics are analyzed and discussed, and comparison between the two fluids are provided. The main conclusions are summarized as follows:

- (1) For both fluids, flow rate has a negligible effect in the thermal performance when nucleate boiling is fully developed, due to the dominance of boiling over convection.
- (2) For TTV1 mimicking a high-performance CPU, R515B provides better thermal performance than R1233zd(E), suggesting higher boiling HTC with R515B. For TTV2 mimicking a high-performance GPU, the two fluids show similar thermal performance, due to the dominance of conduction thermal resistance.
- (3) For both fluids, thermal resistance obtained on TTV1 does not deteriorate at high exit vapor quality >0.8 , but thermal resistance obtained on TTV2 shows heat transfer deterioration when the exit vapor quality exceeds $0.5\sim 0.7$. This is because of the higher heat flux on TTV2 than TTV1 resulting in the occurrence of departure from nucleate boiling or partial dry-out. Geometrical optimization of the cold plate is needed for future improvements.

- (4) The pressure drop of 2P mixture across the vapor QD and its hose connection is much smaller for R515B than for R1233zd(E) due to the difference in vapor density. That indicates higher CDU system level performance using R515B than using R1233zd(E). However, R1233zd(E) is more environmental-friendly and demands less stringent mechanical requirements on the components due to its lower pressure.
- (5) Both R1233zd(E) and R515B offer high performance cooling, and each offers different advantages. Data centers adopting 2P DTC technology can choose between the two fluids by prioritizing mechanical, environmental and performance considerations.

ACKNOWLEDGMENT

The authors thank Aurelio Munoz and Clifford Pauley for their help on experimental setup and testing.

REFERENCES

- [1] A. Heydari, et al. "Experimental evaluation of direct-to-chip cold plate liquid cooling for high-heat-density data centers." *Applied Thermal Engineering* 239 (2024): 122122.
- [2] Q. Wang, R. Chen. "Ultrahigh flux thin film boiling heat transfer through nanoporous membranes." *Nano letters* 18.5 (2018): 3096-3103.
- [3] A. Fazeli, S. Moghaddam. "A new paradigm for understanding and enhancing the critical heat flux (CHF) limit." *Scientific reports* 7.1 (2017): 5184.
- [4] J. W. Palko, et al. "Extreme two-phase cooling from laser-etched diamond and conformal, template-fabricated microporous copper." *Advanced Functional Materials* 27.45 (2017): 1703265.
- [5] K. P. Drummond, et al. "A hierarchical manifold microchannel heat sink array for high-heat-flux two-phase cooling of electronics." *International Journal of Heat and Mass Transfer* 117 (2018): 319-330.
- [6] C. Woodcock, et al. "Ultra-high heat flux dissipation with Piranha Pin Fins." *International Journal of Heat and Mass Transfer* 128 (2019): 504-515.
- [7] A. Narayanan, Q. Wang, S. Ozguc, R. W. Bonner. "Investigation of Server Level Direct-to-Chip Two-Phase Cooling Solution for High Power GPUs." *International Electronic Packaging Technical Conference and Exhibition. American Society of Mechanical Engineers*, 2024.
- [8] D. Kulkarni, et al. "Thermal Performance of Common Cold Plate for Pumped Single- and Two-Phase Direct Liquid Cooling for Next Generation High Power Server Processors." *International Electronic Packaging Technical Conference and Exhibition. American Society of Mechanical Engineers*, 2024.
- [9] D. Kulkarni, et al. "2P Refrigerant-Based Direct Liquid Cooling (DLC) Technology for Next Generation AI Clusters with High TDP Accelerators." *OCF White Paper*.
- [10] Q. Wang, D. P. Kulkarni, R. W. Bonner, J. C. Gulick. "Universal Direct-to-Chip Cold Plates for Single- and Two-Phase Cooling." *2024 OCP Global Summit, Future Technologies Symposium*.
- [11] Q. Wang, R. W. Bonner, "High-Performance Two-Phase Cooling under Different Cold Plate Orientations." *2025 OCP EMEA Summit, Future Technologies Symposium*.
- [12] N. Karwa, S. Y. Motta. "Low-pressure heat transfer fluids for pumped two-phase cooling." *2021 20th IEEE Intersociety Conference on Thermal and Thermomechanical Phenomena in Electronic Systems (iTherm)*. IEEE, 2021.
- [13] Q. Wang, S. Ozguc, A. Narayanan, R. W. Bonner. "A Server-Level Test System for Direct-To-Chip Two-Phase Cooling of Data Centers Using a Low Global Warming Potential Fluid." *2024 23rd IEEE Intersociety Conference on Thermal and Thermomechanical Phenomena in Electronic Systems (iTherm)*. IEEE, 2024.

- [14] A. Heydari, et al. "System-Level Assessment of Green Refrigerant Replacements for Direct-to-Chip Two-Phase Cooling." 2024 23rd IEEE Intersociety Conference on Thermal and Thermomechanical Phenomena in Electronic Systems (iTherm). IEEE, 2024.
- [15] S. Ozguc, Q. Wang, A. Narayanan, J. Moore, R. W. Bonner. "Design Optimization of Manifold Integrated Skived Cold Plates for Two-Phase Flow-Boiling." 2025 41st Semiconductor Thermal Measurement, Modeling & Management Symposium (SEMI-THERM). IEEE, 2025.
- [16] Q. Wang, S. Ozguc, R. W. Bonner. "A Practical Metric for Cold Plate Thermal Performance in Two-Phase Direct-to-Chip Cooling." 2025 41st Semiconductor Thermal Measurement, Modeling & Management Symposium (SEMI-THERM). IEEE, 2025.
- [17] S. G. Kandlikar, et al. Heat transfer and fluid flow in minichannels and microchannels. Elsevier, 2005.
- [18] S. Ozguc, Q. Wang, A. Narayanan, R. W. Bonner. "Investigation of Flow Restrictors for Rack Level Two-Phase Cooling Under Nonuniform Heating." 2024 40th Semiconductor Thermal Measurement, Modeling & Management Symposium (SEMI-THERM). IEEE, 2024.
- [19] S. Ozguc, Q. Wang, A. Narayanan, R. W. Bonner. "Mitigating Flow Maldistribution in Data Center Two-Phase Cooling Systems with Flow Restrictors." Electronics Cooling, Winter 2024.